



Queensland University of Technology
Brisbane Australia

This is the author's version of a work that was submitted/accepted for publication in the following source:

[Liu, Haibo](#), Chen, Tianhu, Chang, Dongyin, Chen, Dong, Xie, Jingjing, & [Frost, Ray L.](#)

(2014)

Effect of palygorskite clay on pyrolysis of rape straw : an in situ catalysis study.

Journal of Colloid and Interface Science, 417, pp. 264-269.

This file was downloaded from: <http://eprints.qut.edu.au/65742/>

© Copyright 2013 Elsevier Inc.

NOTICE: this is the author's version of a work that was accepted for publication in *Journal of Colloid and Interface Science*. Changes resulting from the publishing process, such as peer review, editing, corrections, structural formatting, and other quality control mechanisms may not be reflected in this document. Changes may have been made to this work since it was submitted for publication. A definitive version was subsequently published in *Journal of Colloid and Interface Science*, [Volume 417, (1 March 2014)] DOI: 10.1016/j.jcis.2013.11.041

Notice: *Changes introduced as a result of publishing processes such as copy-editing and formatting may not be reflected in this document. For a definitive version of this work, please refer to the published source:*

<http://doi.org/10.1016/j.jcis.2013.11.041>

1 **Effect of palygorskite clay on pyrolysis of rape straw: an in-situ catalysis**
2 **study**

3

4 **Haibo Liu^{a, b}, Tianhu Chen^{a,*}, Dongyin Chang^a, Dong Chen^a, Jingjing Xie^a,**
5 **Ray L. Frost^{b,*}**

6

7 ^a School of Resource and Environmental Engineering, Hefei University of Technology, China

8

9 ^b School of Chemistry, Physics and Mechanical Engineering, Science and Engineering Faculty,
10 Queensland University of Technology

11

12

* Author to whom correspondence should be addressed

Tel.: +86 13956099615, +86 0551 2903990.

E-mail address: chentianhu@hfut.edu.cn; chentianhu1964@126.com

* Author to whom correspondence should be addressed (r.frost@qut.edu.au)

P +61 7 3138 2407 F: +61 7 3138 1804

13 **Abstract:**

14 Biomass tar restricts the wide application and development of biomass gasification technology.
15 In the present paper, palygorskite, a natural magnesium-containing clay mineral, was
16 investigated for catalytic pyrolysis of rape straw in-situ and compared with the dolomite
17 researched widely. The two types of natural minerals were characterized with XRD and BET.
18 The results showed that combustible gas derived from the pyrolysis increased with an
19 increase of gasification temperature. The $H_{conversion}$ and $C_{conversion}$ increased to 44.7% and 31%
20 for the addition of palygorskite and increased to 41.3% and 31.3% for the addition of
21 dolomite at the gasification temperature of 800 °C, compared with 15.1% and 5.6% without
22 addition of the two types of material. It indicated more biomass was converted into
23 combustible gases implying the decrease of biomass tar under the function of palygorskite or
24 dolomite and palygorskite had a slightly better efficiency than that of dolomite in the
25 experimental conditions.

26

27 **Keywords:** In-situ catalytic cracking, palygorskite clay, dolomite, pyrolysis

28

29

30 1. Introduction

31 Under the pressure to make cleaner less expensive fuels and environmental protection,
32 biomass gasification offers the potential for producing fuel gas that can be used for power
33 generation or synthesis gas applications. Pyrolysis of biomass has several environmental
34 advantages over fossil fuels, such as lower emission of CO₂ and other greenhouse gases [1].
35 However, one of the major issues in biomass gasification is dealing efficiently with tar
36 reduction during the pyrolysis process. This presents a significant impediment to the
37 application of biomass gasification. The condensed compounds present in tar may cause
38 problems in downstream handling, making catalytic hot gas cleaning a necessary step in most
39 gasification applications. Catalytic decomposition appears to be a very attractive way to
40 convert tar components into H₂, CO, etc [2-7].

41
42 Most research has focused on steam reforming of various hydrocarbon feedstock over
43 supported-Ni and expensive metal catalysts [2-5, 8-16]. Furusawa *et al.* [11] reported that
44 Co/MgO catalyst had higher activity than any types of Ni/MgO catalysts. This was attributed
45 to the difference in catalytic performance between Co/MgO and Ni/MgO. In general, Ni
46 catalysts showed high catalytic activity for the removal of tar and are very efficient in tar
47 removal. However, coking on the catalyst surface and sintering of Ni particles caused the loss
48 of the catalytic activity [13]. In addition, to avoid a fast deactivation of Ni catalyst by coke,

49 researchers used CeO₂ as a catalyst additive. It is well known that CeO₂ supported catalysts
50 can promote the reaction of active carbon with O₂ enhancing the catalytic activity and
51 resistance to coking [14-16]. However, these catalysts were difficult to apply in industry due
52 to the carbon deposition and high cost. Therefore, natural minerals, containing dolomite [17-
53 19], olivine [1, 20-23], ilmenite [24], monolith [25], limestone [26] and others, are getting
54 increased attention by many researchers. It has also been reported that the product gas was
55 cleaned and the total product gas yield was increased by using calcined dolomite both in-bed
56 and downstream of a biomass gasifier [17]. Corella *et al.* [23] reported that the use of calcined
57 dolomite inside the gasifier could decrease the tar amount from 6.5 wt% (without dolomite) to
58 1.3 wt%. Rapagna *et al.* [21] investigated the catalytic activity of olivine and observed that it
59 had a good performance in terms of tar reduction. Lopamudra *et al.* [22] investigated effect of
60 the pretreatment of olivine on catalytic cracking of biomass tar. The report of Min *et al.* [24]
61 indicated that ilmenite has good activity for the steam reforming of tar into gases due to its
62 highly dispersed iron-containing species. In short, natural minerals have a catalytic reactivity
63 which may improve the decomposition of biomass tar.

64

65 Besides, palygorskite as a catalyst or catalyst support was investigated in our research
66 [27-30]. The results showed palygorskite was a good catalyst and a better catalyst support for
67 catalytic cracking of biomass tar. However, all the published works concerned the catalytic

68 performance of palygorskite clay by an ex-situ reaction. Palygorskite as an in situ catalyst has
69 never been studied, although it was proved to be a good catalyst and a better catalyst support
70 for decomposition of biomass tar. To improve the gasification efficiency of biomass,
71 palygorskite as an in situ catalyst for catalytic pyrolysis of biomass was investigated and
72 compared with dolomite in the present study. The aim is to investigate the feasibility of
73 palygorskite as an in-situ catalyst for catalytic pyrolysis of biomass and decomposition of
74 biomass tar, and to find a new way for the application of biomass energy—catalytic pyrolysis
75 of biomass using natural mineral, a material with low cost and a large number of storage, and
76 broad the application field of palygorskite clay.

77

78 **2. Experimental**

79 2.1 Materials preparation

80 Palygorskite clay (The formula of the ideal unit cell is $(\text{Mg}, \text{Al},$
81 $\text{Fe})_5\text{Si}_8\text{O}_{20}(\text{OH})_2(\text{OH}_2)_4 \cdot 4\text{H}_2\text{O}$. However, the actual composition of palygorskite varies
82 because of partial replacement of magnesium by aluminum or/and iron) was collected from
83 Guanshan palygorskite clay mine, Mingguang city, Anhui province, China.

84

85 Dolomite ($\text{CaMg}(\text{CO}_3)_2$) was collected from Huaguo mountain, Xuyi county, Jiangsu
86 province, China. The two types of materials underwent drying, crushing and sieving to obtain
87 powder with particles less than 0.075 mm in size. Then, palygorskite clay and dolomite were

88 calcinated at different temperatures (300, 500, 800 °C) for 1 h in flowing nitrogen and cooled
89 to room temperature for further characterization.

90

91 Rape straw was collected around Hefei city, China. The rape straw were smashed and
92 sieved to obtain the particle size lower than 2 mm. The weight percentage of C, H and N was
93 46.83 %, 6.596 % and 0.442 %, respectively, detected before pyrolysis.

94

95 2.2 Materials characterization

96 C, H, N was measured with an element analyzer VARIO ELIII with a high purity of
97 oxygen and a decomposition temperature of 1100°C.

98

99 X-ray diffraction (XRD) was performed using a Rigaku powder diffractometer with Cu
100 $K\alpha$ radiation. The tube voltage was 40 kV, and the current was 100 mA. The XRD diffraction
101 patterns were taken in the range of 5-70° at a scan speed of 4° min⁻¹. Phase identification
102 (Search-Match) was carried out by comparison with those included in the Joint Committee of
103 Powder Diffraction Standards (JCPDS) database.

104

105 13-point BET-nitrogen isotherms were used to quantify changes in the specific surface
106 area. Raw palygorskite and raw dolomite were degassed at 90 °C for 12 h before analysis
107 were conducted. Annealed palygorskite and annealed dolomite were degassed at 150 °C for

108 12h before analysis were conducted. The multi-point BET surface area of each sample was
109 measured at atmospheric pressure using Quantachrome NOVA 3000e Surface Area and Pore
110 Size Analyzer. The adsorption isotherms achieved a p/p_0 range of 0.05-0.35.

111

112 2.2 Testing methods

113 Fig. 1 shows the diagram for in-situ catalytic cracking of rape straw pyrolysis gases with
114 palygorskite or dolomite. The experimental setup involves a sample introduction system, hot
115 cracking system, and detection system. Firstly, the furnace was heated to the desired
116 temperature. Secondly, 10 ± 0.1 g of rape straw was mixed with palygorskite or dolomite and
117 then put into a hopper. Thirdly, carrier gas (160 mL/min), hopper, reaction tube (550×30 mm),
118 ice bath (to condensate biomass tar), wetting flow-meter (to detect production gases) and gas
119 chromatograph (GC, to detect combustible gas concentration) were connected and the air
120 tightness was examined. Then the valve of hopper was loosened and then the pyrolysis
121 reaction of rape straw was started. The reaction time was 10 minutes for every experiment.

122

123 To calculate the pyrolysis efficiency, the composition of pyrolysis gases mainly
124 contained H_2 , CO, CH_4 , C_nH_m and little light hydrocarbon after condensation. According to
125 the report [31], hydrogen (H) from dry wood was mainly converted into CH_4 (more than 30%
126 mol of H at 900°C), H_2 (from 9 to 36% mol. from 700 to 1000°C), H_2O , and C_2H_4 . Thus,
127 combustible gases (H_2 , CO and CH_4 except C_2H_4) were detected by a gas chromatograph

128 (GC-7890T) equipped with a C2000 column (2m×4mm) and a thermal conductivity detector
 129 (TCD) with argon as carrier gas to measure H₂, N₂, CO and CH₄. The column temperature,
 130 evaporation chamber temperature, the temperature and bridge current of detector were 70°C,
 131 120°C, 100°C, 100 mA, respectively.

$$132 \quad Total \cdot combustible \cdot gas(TCG, mL / g \cdot straw) = \frac{V_{H_2} + V_{CO} + V_{CH_4}}{10}$$

133 where, V_{H_2} , V_{CO} , V_{CH_4} represented the total volume of H₂, CO, CH₄, which were calculated
 134 from the result of GC and wetting flow-meter after the pyrolysis of 10g rape straw. In
 135 addition, $C_{conversion}$ and $H_{conversion}$ were calculated as follows:

$$136 \quad C_{conversion} (\%) = \left(\frac{V_{(CO+CH_4)}}{22.4} \times 10^{-3} \times 12 \right) / (W_{straw} \times 46.83\%) \times 100\% = \frac{12 \times V_{(CO+CH_4)}}{46.83 \times 22.4}$$

$$137 \quad H_{conversion} (\%) = \left(\frac{2V_{H_2} + 4V_{CH_4}}{22.4} \times 10^{-3} \times 1 \right) / (W_{straw} \times 65.96\%) \times 100\% = \frac{10 \times (2V_{H_2} + 4V_{CH_4})}{65.96 \times 22.4}$$

138 , where V_{CO} represents the CO yield (mL) after pyrolysis and W_{straw} denotes the weight of
 139 rape straw.

140

141 **Insert Figure 1 here**

142

143 3. Results and discussion

144 3.1 XRD characterization

145 Figure 2 represents the XRD patterns of palygorskite and annealed palygorskite (300,
 146 500, 800 °C), where Cps represents counts per second. Three phases can be identified from
 147 these XRD patterns. The peaks at $2\theta=8.44^\circ$, 13.68° , 16.2° , 27.52° , 34.09° were found and

148 identified as palygorskite. The peaks intensity decreased with an increase of annealing
149 temperature and almost disappeared after annealing at 800°C, which should be attributed to
150 the collapse of palygorskite structure under the function of high temperature. The result was
151 in good agreement with these reports [19, 27]. The peaks at $2\theta=20.76^\circ$, 26.67° , 67.34° were
152 observed and attributed to quartz and can be observed after annealing at all temperatures. The
153 peaks at $2\theta=30.88^\circ$, 41.19° , 44.89° , 50.97° , 59.91° were observed and identified as dolomite.
154 The dolomite takes up about 7.5 wt% in the palygorskite clay, which was calculated roughly
155 according to the result of X-ray fluorescence (XRF) which indicated this palygorskite used in
156 the experiments was mainly composed of Al_2O_3 9.4wt%, MgO 9.9 wt%, Fe_2O_3 5 wt% and
157 CaO 2.3wt%. All XRD peaks of dolomite disappeared when the annealing temperature
158 reached 800°C. As is well-known, dolomite possessed catalytic reactivity assigned to the
159 formation of CaO-MgO when the annealing temperature was over 750°C. Therefore, the peak
160 at $2\theta=42.43^\circ$ can be observed and ascribed to MgO and FeO when palygorskite clay was
161 annealed at 800 °C. However, the characteristic reflection of MgO mainly appeared at
162 $2\theta=37^\circ$ and $2\theta=42.47^\circ$, where the reflection at $2\theta=37^\circ$ has the strongest intensity, as shown in
163 Fig. 3. Furthermore, the intensity of reflection at $2\theta=42.47^\circ$ was the strongest in the newly
164 formed reflection. Therefore, the reflection at $2\theta=42.47^\circ$ should be ascribed to the overlap of
165 the reflection of FeO and MgO. Anyway, wustite ($\text{Fe}_{0.942}\text{O}$)formed after heating at 800 °C,
166 which was assigned to the collapse of the palygorskite structure. It is normal for wustite to be

167 observed as Fe can substitute for Mg and/or Al in the structure of palygorskite and the result
168 of XRF also demonstrated the existence of Fe in this palygorskite clay. That is to say, the
169 palygorskite clay used in this study was mainly composed of palygorskite and dolomite
170 (lower than 7.5 wt%).

171

172 **Insert Figure 2 here**

173 Fig. 3 illustrates the XRD patterns of dolomite and annealed dolomite. Two phases were
174 observed from dolomite and annealed dolomite at 300 and 500°C. Two peaks at $2\theta=23.92^\circ$,
175 26.57° were observed and identified as quartz. These peaks at $2\theta=30.78^\circ$, 41.06° were found
176 and identified as dolomite. However, these peaks for dolomite almost disappeared after
177 annealing at 800°C and displaced by two new phases based on the results of XRD patterns.
178 The peak at $2\theta=29.22^\circ$ was attributed to CaCO_3 and the peaks at $2\theta=37^\circ$, 42.47° , 53.37° were
179 attributed to MgO. That is to say, dolomite was unstable and decomposed into CaCO_3 and
180 MgO when anneal temperature reached 800°C, which was consistent with previously reported
181 [32, 33]. Ratko *et al.* [32] reported that dolomite was decomposed at a temperature below
182 800 °C producing a high concentration of carbon dioxide.

183

184

185 3.2 Nitrogen adsorption-desorption characterization

186 The specific surface area (SSA) of palygorskite, dolomite, annealed palygorskite and

187 dolomite is presented in Table 1. Palygorskite and dolomite were annealed at different
 188 temperatures for 1 h before characterization. The SSA of palygorskite experienced a dramatic
 189 decrease with the increase of annealing temperatures. Especially, the SSA of palygorskite was
 190 only 20.5 m²·g⁻¹ after annealing at 800 °C. The change of SSA of palygorskite with increasing
 191 temperature was ascribed to folded channels and the collapse of palygorskite structure, which
 192 was in good agreement with the results of XRD and in line with other reports [34-36]. In
 193 contrast, no obvious change of SSA of dolomite was found after annealing at 300°C and
 194 500 °C. However, the SSA of dolomite increased to 13.4 m²·g⁻¹ after annealing at 800 °C,
 195 which was assigned to the decomposition of dolomite. Under the function of high temperature,
 196 dolomite was decomposed into CaCO₃ and MgO based on the result of XRD and pore
 197 structure was formed due to the release of CO₂ at the same time [32]. Therefore, dolomite had
 198 a larger SSA after annealing at 800°C.

199
 200 Table 1 SSA of palygorskite and dolomite annealed at different temperatures (m²·g⁻¹).

Material	Raw	300°C	500°C	800°C
Palygorskite	213.5	112.9	82.4	20.5
Dolomite	5.3	4.5	3.6	13.4

201
 202 3.3 Effect of pyrolysis temperature

203 Fig. 4 displays the pyrolysis efficiency as a function of pyrolysis temperature without
 204 addition of palygorskite and dolomite. Obviously, TCG volume increased with an increase of

205 pyrolysis temperature due to the endothermic reaction. Almost no H₂ was detected after the
206 pyrolysis of rape straw at 400 or 500°C. However, H₂ volume increased from 9.35 to
207 60.48mL·g⁻¹ when pyrolysis temperature increased from 600 to 800°C. CH₄ volume had the
208 similar change with H₂. Little CH₄ was detected after the pyrolysis of straw at 400 and 500°C,
209 however it increased from 10.63 to 25.42 mL·g⁻¹ when pyrolysis increased from 600 to 800 °C.
210 It has been widely accepted for the enhancement of high temperature for pyrolysis of biomass.
211 In addition, the $H_{conversion}$ and $C_{conversion}$ had an obvious increase with an increase of pyrolysis
212 temperature, as is shown in Fig. 5. The $H_{conversion}$ increased to 15.3% as well as the $C_{conversion}$
213 increased to 9.6% when pyrolysis temperature came to 800 °C. At low pyrolysis temperature,
214 $C_{conversion}$ was higher than $H_{conversion}$ in contrast with the opposite results when pyrolysis
215 temperature was over 600°C. It is obvious that high temperatures provided more energy and
216 made the break of C-H and C-C bond easy. Therefore, high temperature considerably
217 benefited the further pyrolysis of straw, which agrees well with the previously reported [31].

218 **Insert Figs 4 and 5 here**

219 3.4 Effect of the ratio between palygorskite and straw

220 Fig. 6 illustrates the pyrolysis efficiency as a function of palygorskite percentage in the
221 mixtures. The experiments were carried out at an identical pyrolysis temperature of 500 °C.
222 The TCG increased under all ratios when the mixture of palygorskite and straw was put into
223 pyrolysis reactor. Especially, there was a maximum TCG of 79.81mL·g⁻¹ when the

224 palygorskite percentage reached 3% (3 g palygorskite in 100 g straw). However, TCG
225 increased first and then decreased with an increase of the percentage. To eliminate the testing
226 error, several times of repeat testing was taken and the results displayed the similar data. The
227 reason for the best catalytic efficiency at the percentage of 3% was speculated to the effect of
228 heat conductivity due to more palygorskite. Although no direct evidence supported the
229 explanation, it is easy to understand that heat conductivity needed time. Therefore, it would
230 take more time to reach the furnace temperature because of the addition of more palygorskite.
231 Therefore, the percentage of 3% between natural mineral and straw was selected in the
232 following works. Fig. 7 showed the $H_{conversion}$ and $C_{conversion}$ of straw pyrolysis as a function of
233 ratio between palygorskite and straw at the pyrolysis temperature of 500°C. It was observed
234 that $H_{conversion}$ increased with the increase of the palygorskite percentage between palygorskite
235 and straw. However, the fluctuation of $C_{conversion}$ was observed in Fig. 7. The $C_{conversion}$ had a
236 maximum of 8.1% when the percentage reached 3% between palygorskite and straw. The
237 result is consistent with the change of TCG as mentioned above. It indicates that more carbon-
238 containing matter in biomass is converted to gases implying less biomass tar is formed during
239 the gasification process. The more carbon is converted into combustible gases, the better
240 utilization for the biomass in gasification technology. Anyway, the addition of palygorskite
241 clay enhanced the pyrolysis of straw increasing the TCG and $H_{conversion}$ and $C_{conversion}$. Therefore,
242 palygorskite possesses the potential as an in-situ catalyst for the biomass gasification technology.

243
244
245
246
247
248
249
250
251
252
253
254
255
256
257
258
259
260
261
262

Insert Figs 6 and 7 here

As is well-known, thermal treatment temperature affected the SSA and surface physicochemical properties of palygorskite [27]. Thus, the high annealing temperature (800°C) was considered at the same experimental conditions. Compared with the result of pyrolysis reaction without palygorskite, H₂, CH₄ and TCG volume increased in contrast with the decrease of CO volume when the addition of palygorskite annealed at 800 °C, as is shown in Table 2. However, when it is compared with the results where palygorskite annealed at 500 °C was used, H₂, CO, TCG and $C_{conversion}$ have an obvious decrease in contrast to the increase CH₄ volume and $H_{conversion}$, which not sure whether means more biomass tar will be produced in the process of gasification due to the less production of gases but at least improved the gasification efficiency. That is to say, the utilization of palygorskite anneal at 800°C was better than without palygorskite, but was worse than palygorskite annealed at 500 °C. The reason was ascribed to the catalytic reactive and the decrease of specific surface area as the annealing temperature increases to 800 °C. On the other hand, iron oxide would be formed after self-annealing of palygorskite at 800 °C, as shown in Fig. 2 and magnesium oxide and a little of calcium oxide were formed after the self-annealing of dolomite at 800°C. Uddin *et al.* [37] reported that the activity of the iron oxide catalysts for tar decomposition seemed stable with cyclic use but the activity of the catalysts for the water gas shift reaction decreased with

263 repeated use. Other iron-containing catalysts were also investigated [38-40]. This research
 264 indicated iron oxide or iron-containing catalysts had a good catalytic reactivity for removal of
 265 biomass tar. Therefore, the pyrolysis efficiency was still improved after the addition of
 266 palygorskite, despite the decrease of SSA for palygorskite.

267

268 **Table 2 Effect of palygorskite heat treatment temperature on gases volume**

Material	Anneal temperature/°C	Gas volume/(mL·g ⁻¹)					
		H ₂ TCG	CO	CH ₄	<i>H_{conversion}</i>	<i>C_{conversion}</i>	
3%(palygorskite:straw)	500	9.0	70.8	<0.01	79.8	1.2	8.1
	800	6.0	26.1	4.1	36.1	1.9	3.5
Straw	---	0.5	32.1	<0.01	32.5	0.1	3.7

269

270 3.5 A comparison between dolomite and palygorskite

271 Table 3 showed the effect of dolomite and palygorskite on gases volume of straw
 272 pyrolysis. The percentage between palygorskite or dolomite and straw was 3:100. The two
 273 types of materials were annealed at 500 °C for 1 h before use. On the one hand, the addition
 274 of both dolomite and palygorskite clay considerably improved the gasification efficiency,
 275 especially for the pyrolysis temperature of 800 °C, increasing the H₂, CO, CH₄ and TCG
 276 volume. On the other hand, it was observed that TCG, H₂, CO, CH₄ volume after the
 277 pyrolysis of straw with palygorskite were more than that after pyrolysis with dolomite at
 278 500 °C, as is shown in Table 3. When the pyrolysis temperature reached 800 °C, the

279 improvement of palygorskite clay was just slightly better than that of dolomite. In addition,
 280 $H_{conversion}$ and $C_{conversion}$ had an increase after the addition of palygorskite or dolomite when the
 281 reaction temperature was 500°C. What's more important, $H_{conversion}$ and $C_{conversion}$ increased to
 282 44.7 and 30.9% for the addition of palygorskite and increased to 41.3 and 31.3% for the
 283 addition of dolomite at the pyrolysis temperature of 800 °C. The higher pyrolysis temperature
 284 was, the more apparent the improvement of the pyrolysis efficiency of straw. Additionally,
 285 high temperature can better the pyrolysis efficiency and provide enough energy for catalytic
 286 cracking of biomass tar than that at 500 °C. Corella *et al.* [41] and Orio *et al.* [42] extensively
 287 studied the performance of calcined dolomite (CaO·MgO) for hot gasification-gas cleaning.
 288 The results showed anneal dolomite had a good performance for removal of biomass tar.
 289 Meanwhile, the SSA of dolomite increased from 3.6 to 13.4 m²·g⁻¹ when the annealing
 290 temperature increased from 500 to 800°C, as is reported in Table 1. Therefore, the pyrolysis
 291 efficiency was improved apparently after the addition of dolomite. However, the catalytic
 292 reactivity of palygorskite clay is slightly better than that of dolomite in the present studies.
 293

294 **Table 3 Effect of palygorskite and dolomite on gases volume**

Material	Pyrolysis temperature/°C	Gases volume/mL/g·straw				$H_{conversion}$	$C_{conversion}$
		H ₂	CO	CH ₄	TCG		
3% (palygorskite:straw)	500	9.0	70.8	<0.01	90.0	1.2	8.1
	800	187.1	198.9	71.5	457.5	44.7	30.9
3%(dolomite:straw)	500	3.3	28.1	8.4	39.8	2.7	4.2

	800	178.5	210.4	63.3	452.2	41.3	31.3
Straw only	500	0.5	32.1	<0.01	32.5	0.1	3.7
	800	60.5	58.4	25.4	144.3	15.1	9.6

295

296

297 **4. Conclusions**

298 A new way of biomass gasification with palygorskite, a natural mineral with low cost
 299 and abundant storage, was provided. Pyrolysis temperature favored the gasification efficiency
 300 of straw regardless of with or without palygorskite. The addition of palygorskite improved the
 301 catalytic pyrolysis of straw regardless of the ratio between palygorskite and straw and
 302 improved the gasification efficiency of straw. The addition of palygorskite annealed at 800 °C
 303 increased CH₄ and $H_{conversion}$ compared with that annealed at 500 °C, however dramatically
 304 decreased the H₂, CO, TCG and $C_{conversion}$ due to the evident decrease of specific surface area.
 305 In addition, palygorskite and dolomite can dramatically improve the pyrolysis efficiency
 306 regardless of pyrolysis temperature. However, palygorskite had a slightly better efficiency
 307 than that of dolomite in the experimental conditions. This result can provide information on
 308 the potential application of palygorskite in biomass gasification technology to be determined.

309

310 **5. Acknowledgements**

311 This study was financially supported by National Science Foundation of China (NO.
 312 50774027, 41102023), Specialized Research Fund for the Doctoral Program of Higher

313 Education of China (20110111110003). The authors appreciate the financial support.

314 **References**

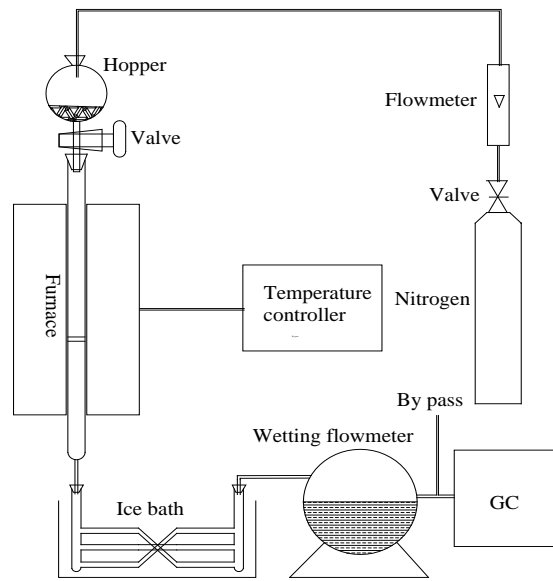
- 315 1. Devi, L., K.J. Ptasinski, and F.J.J.G. Janssen, *A review of the primary measures for tar*
316 *elimination in biomass gasification processes*. *Biomass and Bioenergy*, 2003. **24**(2): p.
317 125-140.
- 318 2. Shie, J.-L., et al., *Catalytic oxidation of naphthalene using a Pt/Al₂O₃ catalyst*. *Applied*
319 *Catalysis B: Environmental*, 2005. **58**(3–4): p. 289-297.
- 320 3. Polychronopoulou, K., C.N. Costa, and A.M. Efstathiou, *The steam reforming of phenol*
321 *reaction over supported-Rh catalysts*. *Applied Catalysis A: General*, 2004. **272**(1–2): p.
322 37-52.
- 323 4. Polychronopoulou, K., J.L.G. Fierro, and A.M. Efstathiou, *The phenol steam reforming*
324 *reaction over MgO-based supported Rh catalysts*. *Journal of Catalysis*, 2004. **228**(2): p.
325 417-432.
- 326 5. Ishihara, A., et al., *Addition effect of ruthenium on nickel steam reforming catalysts*. *Fuel*,
327 2005. **84**(12–13): p. 1462-1468.
- 328 6. Yung, M.M., W.S. Jablonski, and K.A. Magrini-Bair, *Review of catalytic conditioning of*
329 *biomass-derived syngas*. *Energy & Fuels*, 2009. **23**(4): p. 1874-1887.
- 330 7. Li, C. and K. Suzuki, *Tar property, analysis, reforming mechanism and model for*
331 *biomass gasification—An overview*. *Renewable and Sustainable Energy Reviews*, 2009.
332 **13**(3): p. 594-604.
- 333 8. Park, H.J., et al., *Steam reforming of biomass gasification tar using benzene as a model*
334 *compound over various Ni supported metal oxide catalysts*. *Bioresource Technology*,
335 2010. **101 Suppl 1**: p. S101-3.
- 336 9. Ammendola, P., et al., *Rh-perovskite catalysts for conversion of tar from biomass*
337 *pyrolysis*. *Chemical Engineering Journal*, 2009. **154**(1–3): p. 361-368.
- 338 10. Nakamura, K., et al., *Promoting effect of MgO addition to Pt/Ni/CeO₂/Al₂O₃ in the steam*

-
- 339 *gasification of biomass*. Applied Catalysis B: Environmental, 2009. **86**(1–2): p. 36-44.
- 340 11. Furusawa, T. and A. Tsutsumi, *Comparison of Co/MgO and Ni/MgO catalysts for the*
341 *steam reforming of naphthalene as a model compound of tar derived from biomass*
342 *gasification*. Applied Catalysis A: General, 2005. **278**(2): p. 207-212.
- 343 12. Asadullah, M., et al., *A comparison of Rh/CeO₂/SiO₂ catalysts with steam reforming*
344 *catalysts, dolomite and inert materials as bed materials in low throughput fluidized bed*
345 *gasification systems*. Biomass and Bioenergy, 2004. **26**(3): p. 269-279.
- 346 13. Courson, C., et al., *Development of Ni catalysts for gas production from biomass*
347 *gasification. Reactivity in steam- and dry-reforming*. Catalysis Today, 2000. **63**(2–4): p.
348 427-437.
- 349 14. Zhang, R., Y. Wang, and R.C. Brown, *Steam reforming of tar compounds over Ni/olivine*
350 *catalysts doped with CeO₂*. Energy Conversion and Management, 2007. **48**(1): p. 68-77.
- 351 15. Miyazawa, T., et al., *Catalytic performance of supported Ni catalysts in partial oxidation*
352 *and steam reforming of tar derived from the pyrolysis of wood biomass*. Catalysis Today,
353 2006. **115**(1–4): p. 254-262.
- 354 16. Tomishige, K., et al., *Promoting effect of the interaction between Ni and CeO₂ on steam*
355 *gasification of biomass*. Catalysis Communications, 2007. **8**(7): p. 1074-1079.
- 356 17. Pérez, P., et al., *Hot gas cleaning and upgrading with a calcined dolomite located*
357 *downstream a biomass fluidized bed gasifier operating with steam–oxygen mixtures*.
358 *Energy & Fuels*, 1997. **11**(6): p. 1194-1203.
- 359 18. Miao, Y., et al., *Utilization of porous dolomite pellets for the catalytic decomposition of*
360 *acetic acid*. Biomass and Bioenergy, 2010. **34**(12): p. 1855-1860.
- 361 19. Maniatis, K., A.V. Bridgwater, and A. Buekens, *Fluidized bed gasification of wood*, in
362 *Research in Thermochemical Biomass Conversion*, A.V. Bridgwater and J.L. Kuester,
363 Editors. 1988, Springer Netherlands. p. 1094-1105.

-
- 364 20. de Andrés, J.M., A. Narros, and M.E. Rodríguez, *Behaviour of dolomite, olivine and*
365 *alumina as primary catalysts in air–steam gasification of sewage sludge*. Fuel, 2011.
366 **90**(2): p. 521-527.
- 367 21. Rapagnà, S., et al., *Steam-gasification of biomass in a fluidised-bed of olivine particles*.
368 Biomass and Bioenergy, 2000. **19**(3): p. 187-197.
- 369 22. Devi, L., K.J. Ptasinski, and F.J.J.G. Janssen, *Pretreated olivine as tar removal catalyst*
370 *for biomass gasifiers: investigation using naphthalene as model biomass tar*. Fuel
371 Processing Technology, 2005. **86**(6): p. 707-730.
- 372 23. Corella, J., J.M. Toledo, and R. Padilla, *Olivine or dolomite as in-bed additive in biomass*
373 *gasification with air in a fluidized bed: which is better?* Energy & Fuels, 2004. **18**(3): p.
374 713-720.
- 375 24. Min, Z., et al., *Catalytic reforming of tar during gasification. Part I. Steam reforming of*
376 *biomass tar using ilmenite as a catalyst*. Fuel, 2011. **90**(5): p. 1847-1854.
- 377 25. Pfeifer, C. and H. Hofbauer, *Development of catalytic tar decomposition downstream*
378 *from a dual fluidized bed biomass steam gasifier*. Powder Technology, 2008. **180**(1–2): p.
379 9-16.
- 380 26. Weerachanchai, P., M. Horio, and C. Tangsathitkulchai, *Effects of gasifying conditions*
381 *and bed materials on fluidized bed steam gasification of wood biomass*. Bioresource
382 Technology, 2009. **100**(3): p. 1419-1427.
- 383 27. Chen, T., et al., *Effect of thermal treatment on adsorption–desorption of ammonia and*
384 *sulfur dioxide on palygorskite: Change of surface acid–alkali properties*. Chemical
385 Engineering Journal, 2011. **166**(3): p. 1017-1021.
- 386 28. Liu, H., et al., *Catalytic cracking of biomass tar over Ni-based on palygorskite*. Journal
387 of the Chinese Ceramic Society 2011. **39**(4): p. 590-595.
- 388 29. Liu, H., et al., *Effect of Additives on Catalytic Cracking of Biomass Gasification Tar over*

-
- 389 *a Nickel-Based Catalyst*. Chinese Journal of Catalysis, 2010. **31**(4): p. 409-414.
- 390 30. Liu, H., et al., *Effect of preparation method of palygorskite-supported Fe and Ni catalysts*
391 *on catalytic cracking of biomass tar*. Chemical Engineering Journal, 2012. **188**(0): p. 108-
392 112.
- 393 31. Dufour, A., et al., *Synthesis gas production by biomass pyrolysis: Effect of reactor*
394 *temperature on product distribution*. International Journal of Hydrogen Energy, 2009.
395 **34**(4): p. 1726-1734.
- 396 32. Rat'ko, A.I., et al., *Thermal decomposition of natural dolomite*. Inorganic Materials, 2011.
397 **47**(12): p. 1372-1377.
- 398 33. Kók, M.V. and W. Smykatz-Kloss, *Thermal characterization of dolomites*. Journal of
399 Thermal Analysis and Calorimetry, 2001. **64**(3): p. 1271-1275.
- 400 34. VanScoyoc, G.E., C.J. Serna, and J.L. Ahlrichs, *Structural changes in palygorskite during*
401 *dehydration and dehydroxylation*. American Mineralogist, 1979. **64**(1-2): p. 215-223.
- 402 35. Frini-Srasra, N. and E. Srasra, *Effect of heating on palygorskite and acid treated*
403 *palygorskite properties*. Surface Engineering and Applied Electrochemistry, 2008. **44**(1):
404 p. 43-49.
- 405 36. Vágvölgyi, V., et al., *Dynamic and controlled rate thermal analysis of attapulgite*. Journal
406 of Thermal Analysis and Calorimetry, 2008. **92**(2): p. 589-594.
- 407 37. Azhar Uddin, M., et al., *Catalytic decomposition of biomass tars with iron oxide catalysts*.
408 Fuel, 2008. **87**(4-5): p. 451-459.
- 409 38. Nemanova, V., et al., *Biomass gasification in an atmospheric fluidised bed: Tar reduction*
410 *with experimental iron-based granules from Höganäs AB, Sweden*. Catalysis Today, 2011.
411 **176**(1): p. 253-257.
- 412 39. Virginie, M., et al., *Characterization and reactivity in toluene reforming of a Fe/olivine*
413 *catalyst designed for gas cleanup in biomass gasification*. Applied Catalysis B:

-
- 414 Environmental, 2010. **101**(1–2): p. 90-100.
- 415 40. Noichi, H., A. Uddin, and E. Sasaoka, *Steam reforming of naphthalene as model biomass*
416 *tar over iron–aluminum and iron–zirconium oxide catalyst catalysts*. Fuel Processing
417 Technology, 2010. **91**(11): p. 1609-1616.
- 418 41. Corella, J., et al., *Biomass gasification in fluidized bed: where to locate the dolomite to*
419 *improve gasification?* Energy & Fuels, 1999. **13**(6): p. 1122-1127.
- 420 42. Orío, A., J. Corella, and I. Narváez, *Performance of different dolomites on hot raw gas*
421 *cleaning from biomass gasification with air*. Industrial & Engineering Chemistry
422 Research, 1997. **36**(9): p. 3800-3808.
- 423
- 424
- 425

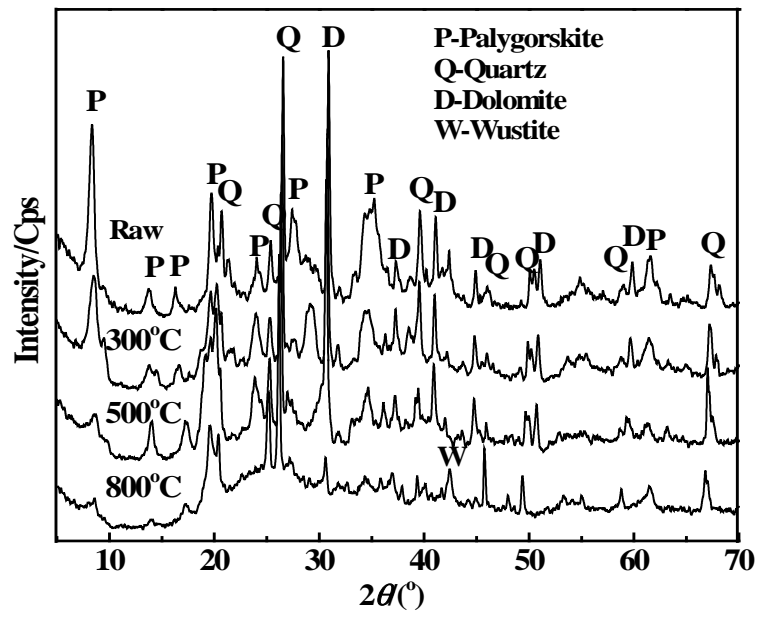


426

427 **Fig. 1. Schematic diagram of in-situ catalytic cracking of rape straw with natural**

428

429

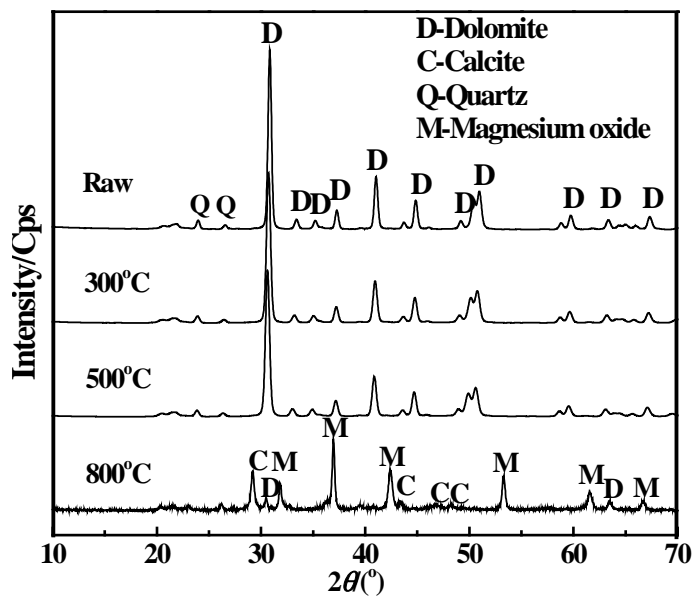


430

431 **Fig. 2 XRD patterns of palygorskite annealed at different temperature.**

432

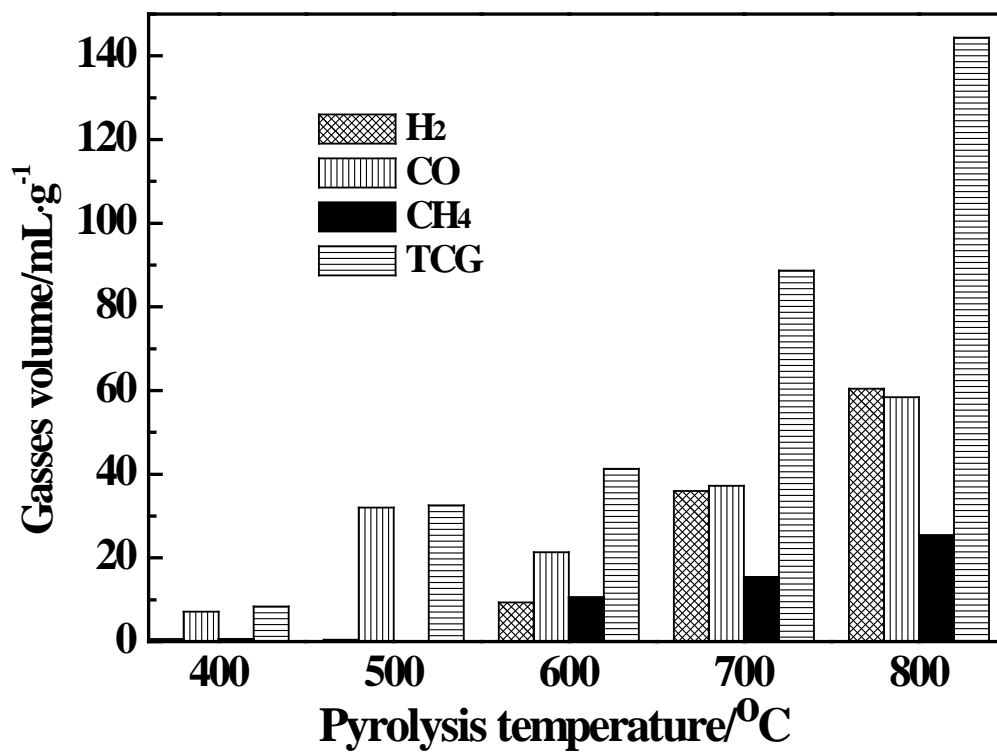
433



434

435 **Fig. 3. XRD patterns of dolomite annealed at different temperatures**

436



438

439

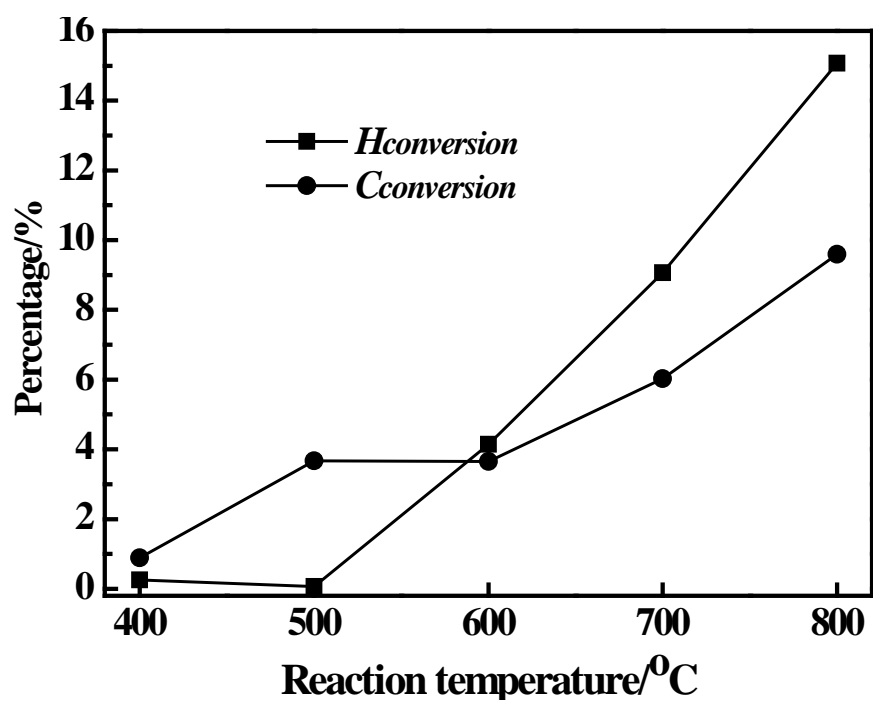
Fig. 4. Effect of pyrolysis temperature on gas volume

440

441

442

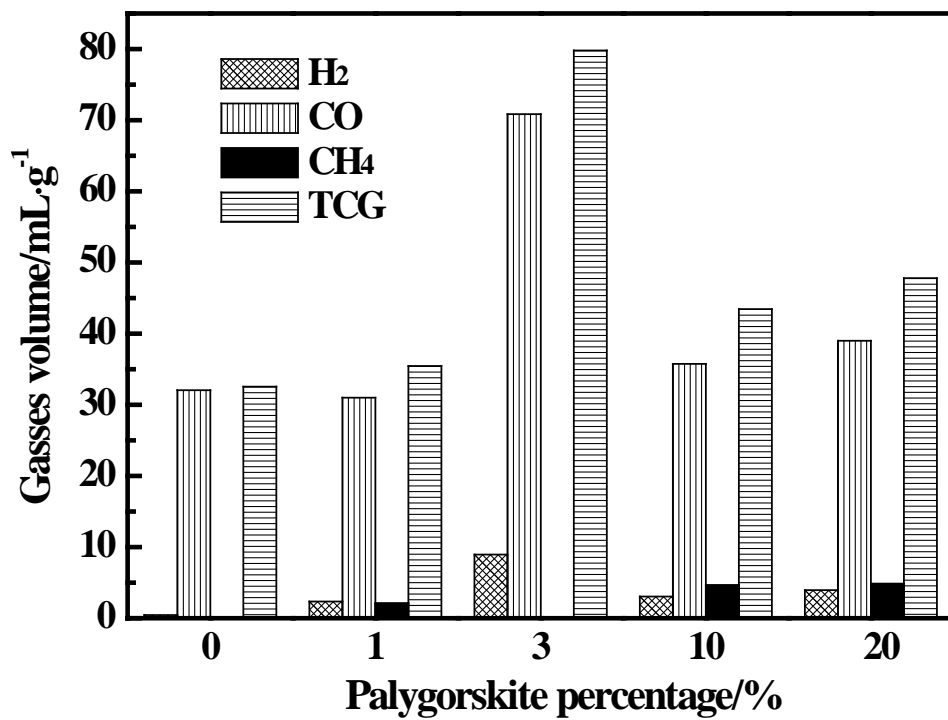
443



444

445 Fig. 5 Effect of pyrolysis temperature on $H_{conversion}$ and $C_{conversion}$

446

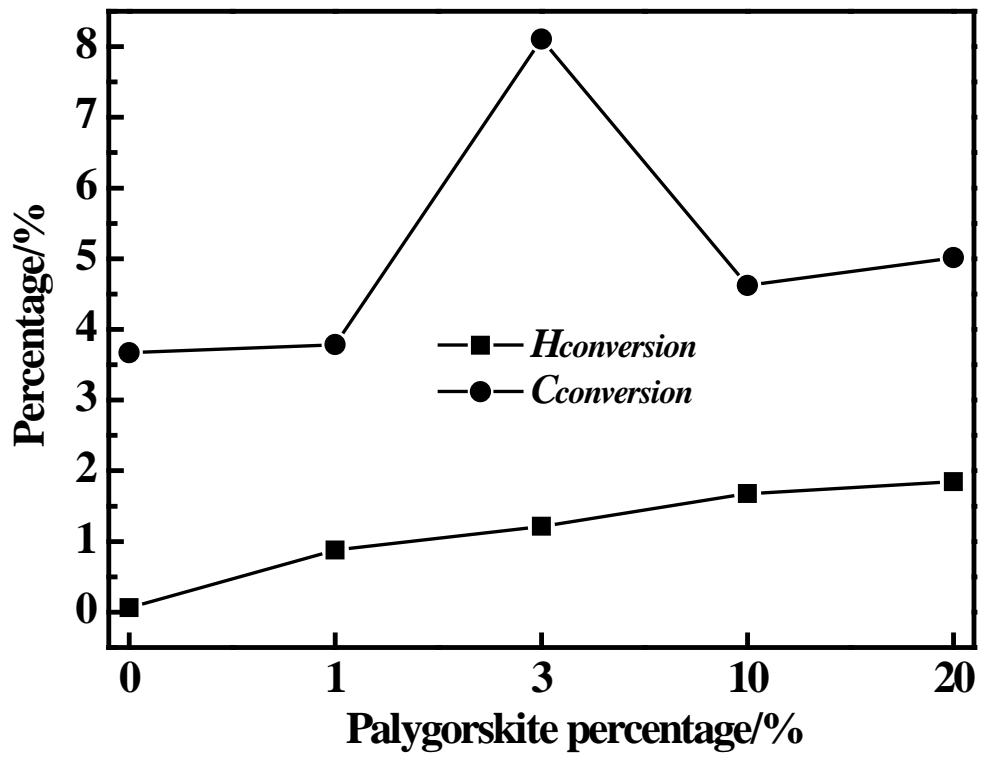


447

448

Fig. 6 Effect of ratio between palygorskite and straw on gases volume

449



450

451 Fig. 7. Effect of Ratio between palygorskite and straw on $H_{conversion}$ and $C_{conversion}$

452

